

Highlights

Fixed-budget optimal designs for multi-fidelity computer experiments

Gecheng Chen and Rui Tuo

- This work introduces a modified autoregressive model to formulate computer code with infinite fidelity levels.
- This work proposes a fixed precision optimal design for the modified autoregressive models.
- This work analyzes the upper bound of the total cost for the proposed MLGP design and compares it with the single fidelity designs.

Fixed-budget optimal designs for multi-fidelity computer experiments

Gecheng Chen and Rui Tuo

Wm Michael Barnes '64 Department of Industrial & Systems Engineering, Texas A&M University, College Station, 77845, Texas, U.S.

Abstract

This work focuses on the design of experiments of multi-fidelity computer experiments. We consider the autoregressive Gaussian process model proposed by Kennedy and O'Hagan (2000) and the optimal nested design that maximizes the prediction accuracy subject to a budget constraint. An approximate solution is identified through the idea of multi-level approximation and recent error bounds of Gaussian process regression. The proposed (approximately) optimal designs admit a simple analytical form. We prove that, to achieve the same prediction accuracy, the proposed optimal multi-fidelity design requires much lower computational cost than any single-fidelity design in the asymptotic sense. Numerical studies confirm this theoretical assertion.

Keywords: Gaussian process models, autoregressive models, multi-level approximation, uncertainty quantification

1. Introduction

With the advance of mathematical modeling and numerical computation, computer simulations have been widely used to mimic complex physical systems. Compared with physical experiments, computer models are often much less costly and more flexible to run. Conceptually, each computer model is based on a mathematical model in terms of, for instance, a set of partial differential equations. The aim of a computer code run is to find a numerical solution to this mathematical model. The design and analysis of computer experiments, an area drawing increasing attention recently, aim to use statistical approaches to collect and analyze computer simulation responses and facilitate decision-making. We refer to the books by Santner et al. (2003); Gramacy (2020) for an introduction to this field. One of the most important tasks in this area is to build *surrogate models*

of computer simulations. A surrogate model is a statistical model constructed using the computer outputs over a selected set of input sites. A point evaluation of a surrogate model is much less costly than running the corresponding computer simulation code. Thus we can use the surrogate model to explore and analyze the underlying computer response function, which expedites the decision-making.

Many computer simulation codes allow users to specify an accuracy level of the numerical responses, in terms of the degree of discretization, or the number of iterations, etc. Generally, there is a trade-off between the accuracy and the computational cost: a high-accuracy computer run is more costly than a low-accuracy run (Qian and Wu, 2008; Xiong et al., 2013). Many statisticians have considered the problem of integrating the computer responses from multiple accuracy (also known as fidelity) levels to make predictions. The first model was suggested by Kennedy and O’Hagan (2000), who proposed a Gaussian-process-based autoregressive model to integrate the output data from computer experiments with multiple fidelity levels. This model has been widely used in real-world applications, e.g., simulation oil pressure (Kennedy and O’Hagan, 2000), designing of linear cellular alloy (Xiong et al., 2013) and prediction of band gaps (Pilania et al., 2017). Alternative models multi-fidelity computer experiments include Bayesian hierarchical models (Qian and Wu, 2008), deep Gaussian process model Cutajar et al. (2019), and nonstationary Gaussian process models (Tuo et al., 2014). In this article, we focus on the autoregressive models given the wide acceptance of these models.

Despite the widespread use of multi-fidelity computer experiments, there remain some unanswered questions. First, it is unclear why one would prefer a multi-fidelity computer experiment over a simple single-fidelity experiment. A conventional explanation says that the low-fidelity data can help explore the underlying response function quickly, and the high-fidelity data are then used to refine the model. This assertion is usually confirmed by numerical studies, but there is a lack of quantitative analysis of this relationship.

The second question is regarding the choice of the set of input sites for the computer simulation, known as a design of experiment. Studying the design of computer experiments is considered important because each computer run can be costly, and a good design can help collect more information under the same computational cost (Santner et al., 2003; Fang et al., 2005). The importance of design of experiments is even more dramatic for multi-fidelity computer experiments, because a poor design can even have an adverse effect on the performance.

A number of designs for multi-fidelity computer experiments are proposed in the literature. Qian (2009) proposed the nested Latin hypercube designs (NLHDs).

The design points of an NLHD on one fidelity level form a Latin hypercube, and those from different fidelity levels are nested. He and Qian (2011) proposed the nested orthogonal array-based Latin hypercube designs to achieve stratification in both bivariate and univariate margins. Rennen et al. (2010) constructed nested maximin Latin hypercube designs using a numerical search algorithm. See also Qian (2009, 2012); Hwang et al. (2016); Qian et al. (2006); Tuo et al. (2014); Xiong et al. (2013); He and Qian (2011); Ehara and Guillas (2021); Sung et al. (2022) for more related works. Despite the rich literature, none of these works addressed the aforementioned questions. Some existing works provided theoretical justifications in terms of numerical integration, e.g., He and Qian (2016), but it is still not clear why these designs are suitable for the autoregressive models.

There is another class of approaches from the area of applied mathematics for a related problem, known as multi-level Monte Carlo (MLMC) (Giles, 2008, 2015; Heinrich, 2001). These methods are algorithms for computing expectations that arise in stochastic simulations with different levels of accuracy. MLMC reduces the computational cost of the traditional Monte Carlo method by taking most samples with low accuracy, and only a few samples taken at high accuracy. Multifidelity Monte Carlo (MFMC) (Ng and Willcox, 2014), based on the control variable techniques for Monte Carlo simulation, resembles the MLMC method for more general engineering models. More related works can be found in Haji-Ali et al. (2016); Peherstorfer et al. (2016a,b); Geraci et al. (2017); Teckentrup et al. (2015). Even though these multi-level based designs are equipped with rigorous mathematical foundations, they are not based on Gaussian process models so that they cannot be used for posterior-based analysis and uncertainty quantification.

This work aims at underpinning the multi-fidelity computer experiments by analyzing their predictive error theoretically. Inspired by the idea of multi-level methods, we formulate a model framework for multi-fidelity computer experiments. We then consider the fixed precision optimal design defined as the design with the minimum total simulation cost subject to an accuracy guarantee. Our main theoretical contribution is to obtain the order of magnitude of the simulation cost as the required predictive error of the autoregressive model goes to zero. The analysis is based on the error bounds for Gaussian process regression provided by Tuo and Wang (2020). We prove that a well-designed multi-fidelity experiment will require much lower simulation cost in the order of magnitude to reach the same accuracy level, compared with the best single-fidelity experiment. This result confirms the superiority of multi-fidelity computer experiments. Based on the theory, we propose a novel design scheme referred to as the multi-level Gaussian process (MLGP) designs. Compared with the existing optimal design methods,

the proposed method is easy to implement because it does not require a numerical search. Numerical studies confirm the superiority of the proposed method over existing alternatives.

The remaining part of this work is organized as follows. Section 2 reviews the autoregressive models. In Section 3, we introduce the formulation of the modified autoregressive model and in Section 4, we introduce the formulation of the modified autoregressive model and propose the MLGP design method. In Section 5, we give the detailed steps for implementing the MLGP method in applications. In Section 6, we conduct some numerical studies, which show the nice performance of the proposed MLGP. The conclusions and some discussion are provided in Section 7. Technical proofs are presented in the Appendix.

2. Review on Gaussian process regression and autoregressive models

In this section, we review the Gaussian process regression and the autoregressive models for multi-fidelity computer experiments.

2.1. Gaussian process regression

Let Z be a Gaussian process on \mathbb{R}^d with mean zero and covariance function $r(x_1, x_2)$. We call Z stationary (Santner et al., 2003) if r can be expressed as a function of $x_1 - x_2$, i.e., $r(x_1, x_2) = \sigma^2 \Phi(x_1 - x_2)$, where σ^2 is the variance, and Φ is a correlation function with $\Phi(0) = 1$; otherwise, we call it nonstationary. Given scattered evaluations $(x_1, Z(x_1)), \dots, (x_n, Z(x_n))$, the Gaussian process regression method (also known as kriging) estimates $Z(x)$ for any $x \in \mathbb{R}^d$ using the conditional expectation

$$\hat{Z}(x) := E(Z(x)|Z(x_1), \dots, Z(x_n)) = a^T(x)R^{-1}Y, \quad (1)$$

where $a(x) := (r(x - x_1), \dots, r(x - x_n))^T$, $R = (r(x_j - x_k))_{jk}$ and $Y = (Z(x_1), \dots, Z(x_n))^T$. In the area of computer experiments, (1) is used to reconstruct the response function $Z(x)$, where $\{x_1, \dots, x_n\}$ denotes the set of designs points, $\{Z(x_1), \dots, Z(x_n)\}$ the corresponding response, and x an untried point.

2.2. Autoregressive model

Kennedy and O'Hagan (2000) proposed a model to fit multi-fidelity computer experiments using Gaussian process regression. The main objective of this model is to incorporate the computer outputs with different fidelity levels and predict the response value of the computer code at an untried point of the highest fidelity level.

Suppose we have K levels of computer codes, with increasing accuracies, denoted as y_1, \dots, y_K . Kennedy and O’Hagan (2000) considered the following autoregressive model to link each pair of consecutive y_i ’s:

$$y_i(x) = \rho_{i-1}y_{i-1}(x) + \delta_i(x), \quad \text{for } i = 2, \dots, K, \quad (2)$$

where ρ_i ’s are known or unknown autoregressive coefficients, and y_1 and δ_t ’s as mutually independent Gaussian processes for all t .

This autoregressive model contains some hyper-parameters. The parameter estimation is usually done using maximum likelihood (Forrester et al., 2007) or Bayesian methods (Kennedy and O’Hagan, 2000). Both approaches involve certain iterative algorithms and thus are expensive in computation. Here we skip the details of the hyper-parameters estimation because they are irrelevant to our main topic. We only consider the prediction for the computer outputs at the highest fidelity given the hyper-parameters. The autoregressive model has been widely used in real-world applications for multi-fidelity computer experiments, e.g., simulation oil pressure (Kennedy and O’Hagan, 2000), designing of linear cellular alloy (Xiong et al., 2013) and prediction of bandgaps (Pilania et al., 2017).

3. Autoregressive models for computer code with infinite fidelity levels

In this work, we focus on computer experiments with infinite fidelity levels. There are many examples of this kind. For example, in finite element analysis, the accuracy is governed by the mesh density, which, at least conceptually, has infinite levels. Other examples include the step length in a finite difference algorithm, the number of iterations in an iterative algorithm, etc. Such a parameter is referred to as a “tuning parameter” in Tuo et al. (2014).

Let us use the finite element method (FEM) as an example to introduce our intuition. FEM generally uses piecewise linear functions over prespecified local patches to approximate general functions, such as the partial differential equation (PDE) solutions. The number of local patches is governed by the chosen mesh size. A typical multi-fidelity computer experiment uses a sequence of consecutively refined meshes. Figure 1 shows the finite elements corresponding to the first three mesh sizes in the set of refining meshes $\{1/2, 1/4, 1/8, \dots, 1/2^n, \dots\}$ in a unit square.

Here comes the question: *what is a suitable configuration of autoregressive models for the above FEM example which can potentially have infinite fidelity levels?* Clearly, we need to make some modifications to (2). The most obvious one

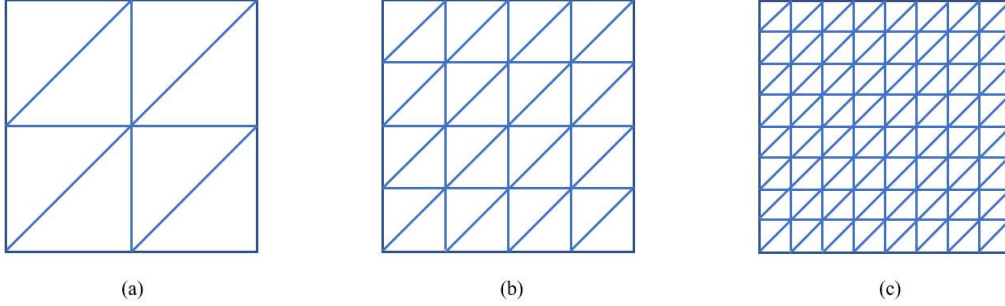


Figure 1: Consecutively refined meshes. The number of the triangle local patches quadruples as the mesh size is halved.

follows from the fact that there are infinite fidelity levels in the above example. That is, conceptually, we should have computer response functions y_i for $i = 1, \dots, K, \dots$. Next, we presume that the FEM solution converges to the exact solution of the PDE as the mesh size goes to zero, which is usually the case. Then the underlying quantity of interest is the function $y_\infty := \lim_{i \rightarrow \infty} y_i$. To guarantee the existence of this limit, more constraints must be imposed in the autoregressive model (2). First, we must have $\lim_{i \rightarrow \infty} \rho_i = 1$ as the existence of y_∞ requires $\lim_{i \rightarrow \infty} (y_i - y_{i-1}) = 0$. In this work, we assume $\rho_i = 1$ for all i for simplicity. Then we have the expression

$$y_\infty = y_1 + \sum_{i=2}^{\infty} \delta_i.$$

Note that $\text{Var}(y_\infty) = \text{Var}(y_1) + \sum_{i=2}^{\infty} \text{Var}(\delta_i)$. To ensure that y_∞ has a finite variance, δ_i must have decreasing variances. Here we model $\delta_i \sim GP(0, \lambda^{2i} \sigma^2 \Phi_i)$ for some correlation function Φ_i , variance σ^2 and $0 < \lambda < 1$. The exponential decay in the variance can be justified because the mesh size in Figure 1 also decays exponentially as the refinement continues. Since we have not seen any data in the experimental design stage, for simplicity, we assume that all the δ_i 's share the same correlation function Φ .

We now define the modified version of the autoregressive model as,

$$y_i(x) = y_{i-1}(x) + \delta_i(x), \quad \text{for } i = 0, \dots, K, \dots, \quad (3)$$

where $y_{-1} = 0$, and $\delta_i \sim GP(0, \lambda^{2i} \sigma^2 \Phi)$ are mutually independent.

4. Multiple fidelity designs based on MLGP

It is hopeful that a multi-fidelity experiment can perform better than a single-fidelity experiment, in the sense that the computational cost is lower to achieve a fixed predictive accuracy. Otherwise, there is no value in using a multi-fidelity design. In this section, the goal is to understand the best prediction performance of a multi-fidelity experimental design.

First, we introduce an assumption for the computational cost of each experimental trial. At the same time, the number of finite elements increases exponentially as the mesh refines iteratively so that the resulting cost for each untried point also increases exponentially. In view of this, we assume the cost for each sample in the i -th level as $C_b a^i \leq C_i \leq C_a a^i$, where C_a and C_b are constants, $a > 1$ is the cost ratio. Additionally, the difference in the approximation values given by successive mesh sizes decreases as the mesh refines.

4.1. A fixed precision optimal design for multi-fidelity models

In this section, we introduce the problem setting for constructing optimal designs for the modified autoregressive model with fixed precision. As discussed in the above section, we use y_∞ to denote the underlying function. (3) allows us to reduce the multi-fidelity problem to a sequence of single-fidelity problems. If we can reconstruct δ_i (i.e., $y_i - y_{i-1}$) for each i , we are able to reconstruct y_∞ using the summation of all these constructed functions. To reconstruct δ_i , a simple idea is to evaluate the function δ_i over a set of selected points, denoted as \mathcal{X}_i correspondingly, via the Gaussian process regression. We assume the underlying function in the K -th layer, i.e., $y_K = \sum_{i=0}^K \delta_i$, is sufficiently accurate. One can reconstruct the y_K by \hat{y}_K defined as (4) to approximate y_∞ .

$$\hat{y}_K(x) = E \left[\sum_{i=0}^K \delta_i(x) \middle| y_K(\mathcal{X}_K), \dots, y_0(\mathcal{X}_0) \right] \quad (4)$$

Denote the desired accuracy level, in terms of the lack of fit, as ϵ ($\epsilon < 1$). Then we can formulate the general objective function for constructing optimal designs for the modified autoregressive model as

$$\min_{n_i, K} \sum_{i=0}^K n_i C_i \quad (5)$$

$$\text{s.t. } E \|y_\infty - \hat{y}_K\|_{L^2}^2 \leq \epsilon^2, \quad (6)$$

where $n_i \in \mathbb{N}$ denotes the sample size of \mathcal{X}_i , and $\|y_\infty - \hat{y}_K\|_{L^2}^2$ is the expected squared predictive error of \hat{y}_K . This objective function can be interpreted as: we want to minimize the cost caused by the designs $\{n_i, K\}$ which satisfies the accuracy requirement.

4.2. MLGP method

The main difficulties for solving (5) include: 1. y_∞ is unknown; 2. \hat{y}_K shown in (4) does not have a closed form under an arbitrary design; 3. the integer optimization problem is NP-hard. In this section, we make some approximations and restrictions to make (5) solvable. In detail, to make the expected squared error in (6) tractable, we only consider nested designs Kennedy and O’Hagan (2001); Qian (2009) to simplify \hat{y}_K . Additionally, we replace the left-hand side of (6) with its upper bound to get an approximated solution. We also relax n_i ’s and K to be real numbers at first to search for the optimal solution, and then round down them to the final optimal solution.

The widely used nested designs can refine the low-accuracy experiments with the high-accuracy experiments to obtain a better model because the response is also available in low-accuracy experiments at the same design points (Qian, 2009). Denote $\mathcal{X}_0, \mathcal{X}_1, \dots, \mathcal{X}_K$ as a sequence of nested sets of points, then the correlation between them can be formulated as $\mathcal{X}_K \subset \dots \subset \mathcal{X}_1 \subset \mathcal{X}_0$. A good property of the nested design given in Theorem 1 helps simplify the approximation (4).

Theorem 1. *Suppose mutually independent $\delta_i \sim GP(0, \sigma^2 \Phi_i)$, $i = 0, 1, \dots, K$, where σ^2 is the variance, Φ is the correlation function and $0 < \lambda^2 < 1$. Let $\mathcal{X}_K \subset \dots \subset \mathcal{X}_1 \subset \mathcal{X}_0$ be a sequence of nested sets of points. Then for each x , the estimator $\hat{y}_K(x)$ defined in (4) admits the expression*

$$\hat{y}_K(x) = \sum_{i=0}^K E \left[(y_i - y_{i-1})(x) \middle| (y_i - y_{i-1})(\mathcal{X}_i) \right]. \quad (7)$$

Theorem 1 shows that if a nested design is used, Gaussian process regression for an autoregressive model can be done by solving a set of single-fidelity Gaussian process regression problems. Specifically, (7) is a sum of $K + 1$ GP predictors. Theorem 1 gives us a good incentive to use nested designs, and then the multi-level interpolation approximation (4) can be rewritten as (7).

The next step is to identify the optimal nested designs for the (5). Because \hat{y}_K depends only on y_0, \dots, y_K , we can see that $y_\infty - y_K$ is independent of $y_K - \hat{y}_K$

and therefore,

$$E \|y_\infty - \hat{y}_K\|_{L^2}^2 = E \|y_\infty - y_K\|_{L^2}^2 + E \|y_K - \hat{y}_K\|_{L^2}^2. \quad (8)$$

To achieve the desired accuracy, a simple idea is to bound each of the right-hand side terms of (8) by $\epsilon^2/2$, i.e., we convert the constrain (6) into

$$E \|y_\infty - y_K\|_{L^2}^2 < \epsilon^2/2, \quad (9)$$

and

$$E \|y_K - \hat{y}_K\|_{L^2}^2 < \epsilon^2/2. \quad (10)$$

where (9) reflects the error caused by using y_K to approximate y_∞ and (10) reflects the error caused by the Gaussian process interpolation. Next, we will handle these two parts separately.

First, we focus on (9). Given the modified autoregressive model with shrinking variance, it is easy to compute the upper bound of the error of the left-hand side of (9).

Theorem 2. *Given mutually independent $\delta_i \sim GP(0, \lambda^{2i} \sigma^2 \Phi)$, $i = 0, 1, \dots, K, \dots$, with $0 < \lambda^2 < 1$ and $\sigma^2 > 0$, we have*

$$E \|y_\infty - y_K\|_{L^2}^2 \leq C_l^2 \lambda^{2K} \sigma^2, \quad (11)$$

where $C_l = \sqrt{C_s}/(1 - \lambda)$ is a constant, and C_s is the volume of the region \mathcal{X} .

Based on Theorem 2, it is sufficient to bound the upper bound of the left-hand side of (11) by $\epsilon^2/2$ to make (9) hold, that is,

$$E \|y_\infty - y_K\|_{L^2}^2 \leq C_l^2 \lambda^{2K} \sigma^2 \leq \epsilon^2/2.$$

Then we can choose

$$K = \left\lceil \log_{\lambda^2} \frac{\epsilon^2}{2C_l^2 \sigma^2} \right\rceil, \quad (12)$$

as the total number of levels K , where $\lceil a \rceil$ denotes the largest integer which is smaller or equal to a .

Next, we turn to (10), which is associated with the error from the Gaussian process modeling. Here we make a similar assumption as the Tuo and Wang

(2020) to our nested designs. Before introducing the assumption, we make some definitions. For a set of design points $\mathcal{X} = \{x_1, x_2, \dots, x_n\} \subset \Omega$, define the fill distance as

$$h_{\mathcal{X}, \Omega} = \sup_{x \in \Omega} \inf_{x_j \in \mathcal{X}} \|x - x_j\|,$$

and the separation radius as

$$q_{\mathcal{X}} = \min_{1 \leq j \neq k \leq n} \|x_j - x_k\|/2.$$

Assumption 1. $\mathcal{X}_K \subset \dots \subset \mathcal{X}_1 \subset \mathcal{X}_0$ is a sequence of nested sets of points, denote the corresponding fill distance and separation radius as $h_{\mathcal{X}_i, \Omega}$ and $q_{\mathcal{X}_i}$. There exists a constant A such that $h_{\mathcal{X}_i, \Omega}/q_{\mathcal{X}_i} \leq A$ holds for all i .

Given scattered evaluations $(x_1, Z(x_1)), \dots, (x_n, Z(x_n))$ where the design is quasi-uniform, if we use the Matérn kernel to reconstruct the underlying function $Z(x)$, then there exist two positive constants p and q such that Tuo and Wang (2020):

$$E \left\| Z(x) - \hat{Z}(x) \right\|_{L^2}^2 < pn^{-2\nu/d}, \quad (13)$$

and

$$E \left\| Z(x) - \hat{Z}(x) \right\|_{L^2}^2 > qn^{-2\nu/d}, \quad (14)$$

where $\hat{Z}(x)$ is the reconstructed function, ν is the smoothness parameter of the Matérn kernel and d is the dimension of the design.

Based on the error bound of the original Gaussian process regression, we propose the upper bound of the interpolation error in the modified autoregressive model in Theorem 4.

Theorem 3. Assume a infinite series $\delta_i \sim GP(0, \lambda^{2i} \sigma^2 \Phi)$ and they are mutually independent. Denote y_K as the summation of the first $(K + 1)$ terms, and \hat{y}_K defined in (7) as the emulation of y_K based on the set of points \mathcal{X}_i and Matérn kernel, then under Assumption 1 we have

$$E \left\| y_K - \hat{y}_K \right\|_{L^2}^2 \leq \sum_{i=0}^K p \lambda^{2i} \sigma^2 n_i^{-2\nu/d}, \quad (15)$$

where n_i is the number of points of X_i , d is the number of dimension, p is a constant, ν is the smoothness parameter of Φ .

Based on Theorem 4, it is sufficient to bound the upper bound of the left-hand side of (16) by $\epsilon^2/2$ to make (10) hold. Then we can approximate the solution of the objective function (5). Based on Tuo and Wang (2020), we state the upper bound of the interpolation error in the modified autoregressive model in Theorem 4.

Theorem 4. *Assume a infinite series $\delta_i \sim GP(0, \lambda^{2i}\sigma^2\Phi)$ and they are mutually independent. Denote y_K as the summation of the first $(K + 1)$ terms, and \hat{y}_K defined in (7) as the emulation of y_K based on the set of points \mathcal{X}_i and Matérn kernel, then under Assumption 1 we have*

$$E \|y_K - \hat{y}_K\|_{L^2}^2 \leq \sum_{i=0}^K p\lambda^{2i}\sigma^2 n_i^{-2\nu/d}, \quad (16)$$

where n_i is the number of points of X_i , d is the number of dimension, p is a constant, ν is the smoothness parameter of Φ .

Based on Theorem 4, it is sufficient to bound the upper bound of the left-hand side of (16) by $\epsilon^2/2$ to make (10) hold. Then we can approximate the solution of objective function (5) with (6) by solving a relaxed version, i.e.,

$$\begin{aligned} \min_{n_i} \quad & \sum_{i=0}^K n_i C_i \\ \text{s.t.} \quad & \sum_{i=0}^K p\lambda^{2i}\sigma^2 n_i^{-2\nu/d} \leq \epsilon^2/2 \end{aligned} \quad (17)$$

where $K = \lceil 2 \log_{\lambda^2} \frac{\epsilon}{2C_1\sigma} \rceil$. One can see that (17) is an integer programming problem which is NP-hard. In view of this, we consider a relaxed version of it. First we assume n_i 's can choose any real number, then (17) becomes a convex optimization problem whose optimal solution is

$$n_i = \left(\frac{\epsilon^2}{2p\sigma^2 S} \right)^{-\frac{d}{2\nu}} \left(\frac{a^i}{\lambda^{2i}} \right)^{-\frac{d}{d+2\nu}}, \quad i = 0, \dots, K, \quad (18)$$

where $S = \sum_{i=0}^K (a^i)^{\frac{\nu}{d+2\nu}} (\lambda^{2i})^{\frac{d}{d+2\nu}}$, p is a constant. The proof of (18) is given in the Appendix.

Note that $\lceil n_i \rceil$'s also locate in the feasible region of (17). We regard the $\lceil n_i \rceil$'s

shown in (19) as a nearly optimal solution to (17).

$$n_i = \left\lceil \left(\frac{\epsilon^2}{2p\sigma^2 S} \right)^{-\frac{d}{2\nu}} \left(\frac{a^i}{\lambda^{2i}} \right)^{-\frac{d}{d+2\nu}} \right\rceil, \quad i = 0, \dots, K, \quad (19)$$

In summary, we consider the designs generated based on (19) and (12) as the optimal designs for the modified autoregressive model. We will discuss the implementation details in Section 5.

4.3. Comparison with single-fidelity experiments

In this section, we will show that the MLGP needs less cost than any single-level method to achieve a given accuracy provided that the accuracy level is small enough. Let us denote $a = \exp(\alpha)$ and $\lambda^2 = \exp(-\beta)$ for convenience ($\alpha, \beta > 0$). In this section, we use the symbol “ \lesssim ” to represent that the left-hand side is less than the right-hand side multiplied by a constant depending only on Φ . First, we give an upper bound for the total cost for the MLGP method that reaches a fixed accuracy level ϵ .

Theorem 5. *Assume $y_i(x) = y_{i-1}(x) + \delta_i(x)$, for $i = 0, \dots, K, \dots$, where $\delta_i \sim GP(0, \lambda^{2i} \sigma^2 \Phi)$ and they are mutually independent, $\lambda^2 < 1$ and $y_{-1} = 0$. If we use the design (12) and (19) to reach a fixed accuracy level ϵ , then the upper bound for the total cost is summarized as*

$$C_\epsilon \lesssim \begin{cases} \epsilon^{-d/\nu}, & 2\alpha\nu < d\beta \\ \epsilon^{-d/\nu} |\ln \epsilon^2|^{\frac{d+2\nu}{2\nu}}, & 2\alpha\nu = d\beta \\ \epsilon^{-2\alpha/\beta}, & 2\alpha\nu > d\beta \end{cases} \quad (20)$$

Next, we discuss the lower bound for the total cost if we implement the single-fidelity method to reach the accuracy level ϵ .

Theorem 6. *Assume $y_i(x) = y_{i-1}(x) + \delta_i(x)$, for $i = 0, \dots, K, \dots$, where $\delta_i \sim GP(0, \lambda^{2i} \sigma^2 \Phi)$ and they are mutually independent, $\lambda^2 < 1$ and $y_{-1} = 0$. If we only spread design samples in one layer to reach a fixed accuracy level ϵ , then the lower bound for the total cost is*

$$C_\epsilon^{SL} \gtrsim \epsilon^{-\left(\frac{d}{\nu} + \frac{2\alpha}{\beta}\right)}. \quad (21)$$

5. Fixed budget designs

For many real applications, a more realistic assumption is that the total budget, rather than the accuracy level, is fixed. In this section, we will introduce how to implement the MLGP design method given a fix budget.

First, assume we know the values for the hyper-parameters λ^2 , correlation function, and ν . In practice, λ^2 can be decided based on expert knowledge. For example, we can choose the decreasing ratio of the mesh sizes as λ^2 in the FEM case. The correlation function and the corresponding parameter(s) need to be decided based on the smoothness of the underlying function, see Wilson and Adams (2013); Schulz et al. (2018) for more information.

In order to obtain the designs based on (12) and (19) under a certain budget B , we need to have the exact values for the parameters p , C_l , σ and the desired accuracy level ϵ . These parameters are often hard to decide in real-world applications. However, the number of available layers is often determined in real-world applications. Based on this, we just assume K is determined. Please note that this assumption does not mean we need to use all the layers in our designs because n_i can be very small for a certain layer if the MLGP method thinks that the corresponding layer is not needed.

The next thing is to calculate n_i . Denote $\tau := p\sigma^2/\epsilon^2$ and $\eta := p/C_l^2$, then we rewrite (19) as

$$n_i = \left\lceil (2\tau S)^{\frac{d}{2\nu}} \left(\frac{a^i}{\lambda^{2i}}\right)^{-\frac{d}{d+2\nu}} \right\rceil, \quad i = 0, 1, \dots, K \quad (22)$$

where $\tau = \frac{\eta}{2\lambda^{2K}}$.

In order to avoid the estimation of those constants (p , C_l , σ and ϵ), one can tune η to get the corresponding optimal design under the fixed budget B . By choosing a value for η , we can get a value for τ which leads to corresponding $n_i, i = 0, \dots, K$ according to (22). The resulting design that triggers the highest cost and meets the budget requirement can be chosen as the optimal design n_i^* 's. In applications, the user can try different values for η in a pre-specified set (e.g., the integers from 1 to 100) to search for the optimal design n_i^* 's.

Note that the design n_i^* 's does not use all the budget in most cases because we need to choose an integer for n_i^* 's when implementing (22). Denote the unallo-

cated budget as

$$B_K = B - \sum_{i=0}^K n_i^* C_i. \quad (23)$$

The final step is to re-allocate B_K to modify the design $n_i^*, i = 0, \dots, K$. We implement a greedy algorithm to solve the following objective function (24) to re-allocate the budget to further reduce the error in the left-hand side of the constraint of (17).

$$\min_{n_i^{**}} \quad \sum_{i=0}^K \lambda^{2i} \sigma^2((n_i^{**})^{-2\nu/d} - (n_i^*)^{-2\nu/d}) \quad (24)$$

$$\text{s.t.} \quad \sum_{i=0}^K (n_i^{**} - n_i^*) C_i \leq B_K \quad (25)$$

Then we get the final optimal designs $n_i^{**}, i = 0, \dots, K$.

Denote a K level design as a vector $N = [n_1, \dots, n_K]$, and a function $G(N^{**}) = \sum_{i=0}^K \lambda^{2i} \sigma^2((n_i^{**})^{-2\nu/d} - (n_i^*)^{-2\nu/d})$. Also denote a vector with the i -th element equal to 1 and other elements equal to 0 (i.e., $1^i = [0, \dots, 1, \dots, 0]$) as one sample in the i -th layer. Now the detailed steps of the re-allocating starting from the design N^* are as follows:

- Search i exhaustively in the range $[0, K]$ to minimize $G(N^* + 1^i)$ on the condition that $C_i \leq B_K$;
- Add one sample to the i -th layer of N^* , that is, $N^* = N^* + 1^i$;
- Calculate the unallocated budget $B_K = B_K - C_i$;
- Repeat the above steps until $B_K = 0$ or B_K cannot afford any additional sample.

Remark 1. Before reaching the optimal designs, we need to determine the values for several parameters, including $a, C_a, C_b, B, K, \lambda, \nu$ and η . Some of the parameters are given or estimated by specific applications, such as a, C_b, C_a, B and K . Some of the parameters need to be chosen by the users based on experience or other knowledge, i.e., λ and ν . We may misspecify them because we do not know the true values for these two parameters. However, empirical studies show that the designs generated by the proposed MLGP can still outperform existing alternatives even with misspecified values. See Section 6.2 for more details. As for the tuning of η , screening only over integer values should give decent tuning

results. Note that we still have a re-allocation step after this search that will further modify the design, so we still have a good chance to get a nice design even if we do not reach the optimal η exactly. If need, when the optimal η lies between two consecutive integers, we can consider a finer discretization over the search space to obtain a better η . Besides, some other searching methods are available to find the optimal η more efficiently, such as the binary search algorithm which is applied in our experiments.

Given the detailed steps for calculating the n_i^{**} 's for each layer, we still need to decide how to spread these samples in each layer. Please recall that the error bound in Theorem 4 only holds when Assumption 1 holds. But it is very hard to maintain this assumption in applications rigorously because it involves a lot of optimization steps. we consider approximately space-filling sequences, such as Halton sequences (Halton, 1964) which is a type of low-discrepancy sequences. Halton sequences enjoy the following two advantages. First, it can give designs of any sample sizes. Second, the sequences have analytical expressions which are easy to compute.

5.1. Examples

In this section, we visualize the designs generated by the MLGP under different budgets or different λ^2 in $[0, 1]^2$. We choose $a = 4$ and $C_a = C_b = 1$ for the experiments in this section.

In the first experiment, we use $B = 192$, $K = 2$ and Matérn correlation function with $\nu = 1.25$ to generate designs under four different λ^2 using the MLGP. Tabel 1 and Figure 2 show the design structures when λ^2 changes from $1/8$ to $3/4$. Note that the column "Design structure" shows the number of samples from the lowest to the highest layer. For example, the design 20, 7, 3 means a nested design with 20 samples (empty circles in Figure 2) in the 0-th layer, 7 samples (filled circles in Figure 2) in the 1st layer and 3 samples (filled triangles in Figure 2) in the 2nd layer. The subplot a, b, c and d are corresponding to $\lambda^2 = 1/8$, $\lambda^2 = 1/4$, $\lambda^2 = 1/2$ and $\lambda^2 = 3/4$, respectively. It can be seen that the MLGP allocates more budget on the higher layers with the λ^2 increases. This phenomenon exactly matches the changing of the true function. This is because the variance of δ_i 's in (7) in the high layers take less proportion in the underlying function y_K if λ^2 is small. In other words, the information of the higher layers plays a less important role in the overall accuracy. As a result, if we want to get a low error as much as possible under a fixed budget, we should pay more budget on the samples in the lower layers and vice versa. This exclusive flexibility of the

MLGP can help the users a lot to construct suitable designs when facing different λ^2 while the multi-level and single-level methods can only build designs with fixed proportions.

In the second experiment, we use $K = 2$, $\lambda^2 = 1/2$, Matérn correlation function with $\nu = 1.25$ to generate designs under budgets from 96 to 240 using the MLGP. Table 2 and Figure 3 show the design structures generated by the MLGP under different B .

In the third experiment, we test our method under large ν 's for the Matérn correlation function. We use $K = 3$, $\lambda = 1/2$ and budget $B = 4760$ to generate designs under different ν 's from 5 to 50. Table 3 shows the designs in this experiment, we can see that our method still works well under large ν 's.

Table 1: Designs under different λ^2

λ^2	Design structure
1/8	48, 16, 5
1/4	32, 16, 6
1/2	24, 14, 7
3/4	16, 12, 8

Table 2: Designs under different budgets B

B	Design structure
96	20, 7, 3
144	24, 10, 5
192	24, 14, 7
240	28, 17, 9

Table 3: Designs under different smoothness parameters ν

ν	Design structure
5	24,16,16,7
10	16, 9, 17, 7
25	16, 9, 9, 8
50	16, 9, 9, 8

6. Numerical study

In this section, some numerical studies will be conducted to show the superiority of the proposed MLGP. In Section 6.1, we will first compare the performance of the proposed MLGP, classical multi-fidelity designs, and single-level designs in 1-dimensional cases when we know all hyper-parameters (λ^2 , correlation function, and ν). Then we will test the performance of these three methods if one of the hyper-parameters is misspecified in Section 6.2. In Section 6.4, we will compare the proposed MLGP with Nested Latin Hypercube designs and single-level

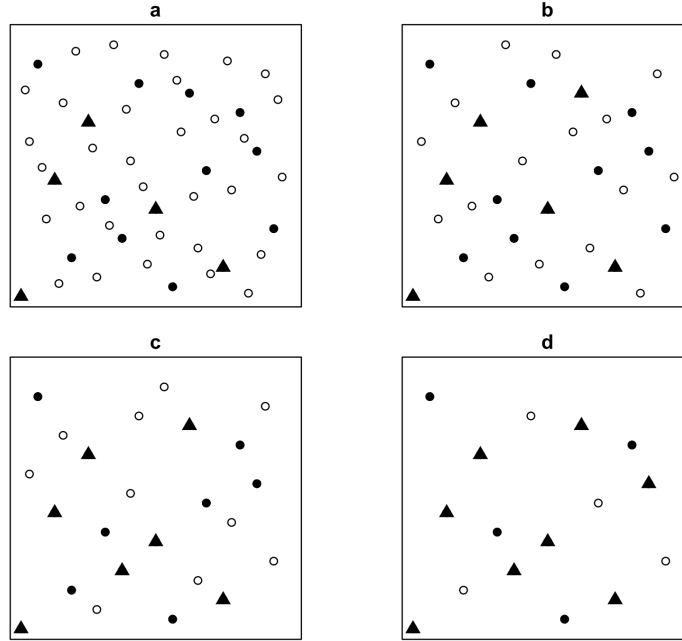


Figure 2: Designs generated by MLGP under different λ^2

designs in a 2-dimensional case. Emulators given by the proposed MLGP yield more accurate results than other methods in all cases.

6.1. Numerical study in one-dimensional space

In the section, we prepare a four-level function $f(x)$ (i.e., $K = 3$) defined in $[0, 15]$ as the simulation function. Each level is assumed as a mutually independent Gaussian process with zero mean and Matérn correlation function. We assume $\lambda^2 = 1/3$, the correlation matrix is Matérn correlation function with $\nu = 1.25$. In this experiment, we choose the cost ratio $a = 8$ and the cost for each sample in the 0-th layer to be 1, i.e., $C_a = C_b = 1$.

In this experiment, we assume all the true values hyper-parameters are known. We calculate three groups of designs based on the proposed MLGP method, the classical multi-fidelity design method, and the single-level design method under different budgets. After calculating the number of samples in each layer, we generate the corresponding (nested) design samples based on the Halton sequences for all three methods. Then we train a Gaussian process regression (GPR) emulation based on each design to test the prediction accuracy on a testing set with 200 samples. Note that we do not use maximum likelihood estima-

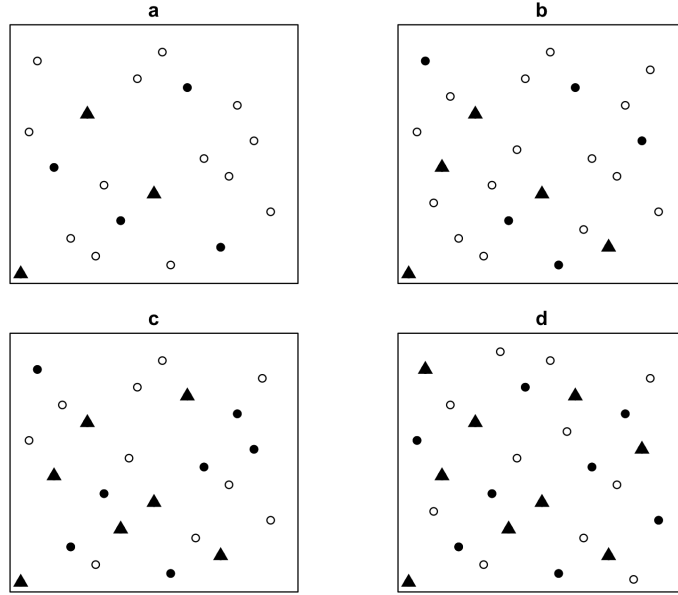


Figure 3: Designs generated by MLGP under different budgets B

tion (MLE) to estimate the variance and the length parameter. The accuracy of GPR emulations is measured by the root mean squared error (RMSE) defined as $RMSE = \sqrt{N^{-1} \sum_{i=1}^N (y_i - \hat{y}_i)^2}$, where $N = 200$, y_i , and \hat{y}_i are the true label and the predictive label for the i -th testing sample, respectively.

In order to make the results more convincing and show the robustness of the proposed MLGP algorithm, we repeat this experiment 30 times starting from different realizations of $f(x)$ and compare the mean RMSE of these methods.

Figure 4 shows the average RMSEs of the three methods under different budgets. The blue line shows the performance of the single-level method, and it almost keeps the same even with different budgets. This is because in all cases, the best accuracy of the single-level method is achieved by only sampling at the 2-th layer. The red line and the black line represent the performance of the multi-level method and the MLGP, respectively. One can easily see that the designs given by the MLGP lead to the emulations with the lowest RMSEs compared with other methods, which proves the superiority of the proposed MLGP.

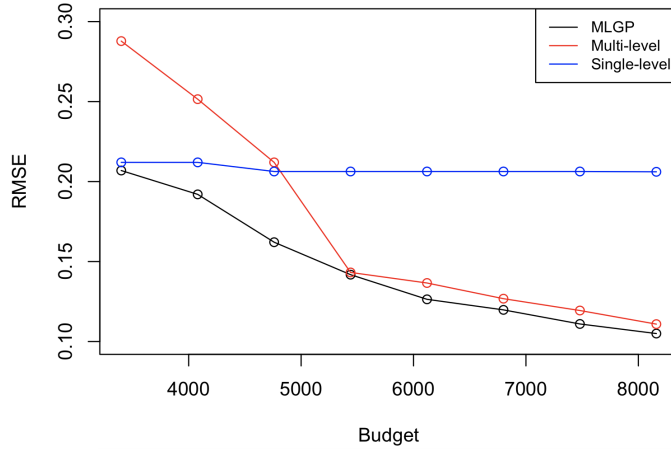


Figure 4: RMSEs of the MLGP, classical multi-fidelity method and single-level method for the 1-dimensional case under different budgets.

6.2. Numerical study for the situations with misspecified hyper-parameters

We may not get the exact values for all the hyper-parameters in some cases. To show the robustness of the MLGP, we also test the performance of the proposed MLGP when we incorporate a misspecified hyper-parameter. First, we use the same parameters as the first experiment to generate the four-level function $f(x)$, i.e., $K = 3$, $\lambda^2 = 1/3$, Matérn correlation function with $\nu = 1.25$. Also, we choose the cost ratio $a = 8$ and $C_a = C_b = 1$. We generate designs based on the proposed MLGP using all the same parameters but a misspecified $\lambda^2 = 1/2$. Then we test the GPR emulation trained by this design and compare the accuracy of the testing set with other methods. Next, we use the hyper-parameters $K = 3$, $\lambda^2 = 1/3$, Matérn correlation function with $\nu = 1.25$ to generate the four-level function $f(x)$ and generate designs based on the proposed MLGP using all the same parameters but a misspecified $\nu = 1.5$. GPR emulation is also used to compare the performance of the MLGP and the other two methods.

Table 4 shows the results for these two experiments. One can see that the MLGP still gets the lowest error even though the misspecified hyper-parameters are incorporated.

6.3. Case study in two-dimensional space

In this section, we will compare the performance of the proposed MLGP, the nested Latin hypercube design (NLHD), and the single-level design in a two-dimensional case. We prepare a three-level function $f(x)$ (i.e., $K = 2$) defined in

Table 4: Mean RMSEs for the proposed MLGP method, classical multi-fidelity design method and single-level design method with misspecified λ^2 or ν

Situation	Method	Average RMSE	Designs structure
misspecified λ^2	MLGP	0.2831	88, 32, 21, 6
	Multi-fidelity	0.3441	56, 28, 14, 7
	Single-level	0.3789	0, 0, 74, 0
misspecified ν	MLGP	0.1652	88, 40, 20, 6
	Multi-fidelity	0.2127	56, 28, 14, 7
	Single level 2	0.2064	0, 0, 74, 0

$[0, 1]^2$ as the simulation function. Each level is assumed as a mutually independent Gaussian process (GP) with zero mean and Matérn correlation function with $\nu = 1.25$. We assume $\lambda^2 = 1/2$. In this experiment, we choose the cost ratio $a = 4$ and the cost for each sample in the 0-th layer to be 1, i.e., $C_a = C_b = 1$.

In this experiment, we assume all the true parameters are known, i.e., $\lambda^2 = 1/2$, the correlation function is Matérn correlation function with $\nu = 1.25$. For the proposed MLGP and single-level methods, we first calculate the design structure and then generate the corresponding (nested) samples using the Halton sequences. As for the NLHD, we use a design given in Table 7. Then we train a GPR emulation based on each design to test the prediction accuracy on a testing set with 500 samples based on the root mean squared error (RMSE). In this experiment, 30 different realizations of $f(x)$ are generated to test the average RMSE of the GPR emulations. Table 5 shows the average RMSEs and the design structures of these three methods. We can see that the MLGP yields the lowest RMSE, which demonstrates the effectiveness of the MLGP in two-dimensional cases.

6.4. Case study in higher dimensional space

In this section, we will compare the performance of the proposed MLGP and the single-level design in four-dimensional and eight-dimensional cases. We prepare a three-level function $f(x)$ (i.e., $K = 2$) defined in $[0, 1]^2$ as the simulation function. Each level is assumed as an i.i.d Gaussian process (GP) with zero mean and Matérn correlation function with $\nu = 1.25$. We assume $\lambda^2 = 1/2$. In this experiment, we choose the cost ratio $a = 4$ and the cost for each sample in the 0-th layer to be 1, i.e., $C_a = C_b = 1$.

Table 5: Results for the proposed MLGP method, Nested Latin hypercube design (NLHD) and single level design method

Method	Average RMSE	Designs structure
MLGP	0.1510	20, 7, 3
Multi-fidelity	0.1735	32, 8, 2
Single-level	0.1658	0, 0, 6

In this experiment, we assume the available budget $B = 144$, $\lambda^2 = 1/2$ and the correlation function is Matérn correlation function with $\nu = 1.25$. For the proposed MLGP and single-level methods, we first calculate the design structure and then generate the corresponding (nested) samples using the Halton sequences. Then we train a GPR emulation based on each design to test the prediction accuracy on a testing set with 500 samples based on the root mean squared error (RMSE). In this experiment, 30 different realizations of $f(x)$ are generated to test the average RMSE of the GPR emulations. Table 7 shows the average RMSEs and the design structures of these two methods. We can see that the MLGP yields the lowest RMSE, which demonstrates the effectiveness of the MLGP in higher dimensional cases.

7. Conclusion

In this work, we propose new experimental designs for multi-fidelity computer experiments, called the multi-level Gaussian process (MLGP) designs, and prove that they are theoretically superior to any single-fidelity designs. In our theoretical analysis, we assume that a quasi-uniform nested design is used. It is not clear how to obtain such a nested design efficiently. Chen and Xiong (2017) proposed a numerical algorithm to search for good nested designs. In our work, we use Halton sequences, which are computationally efficient and nearly quasi-uniform. The proposed designs are readily applicable for a wide range of multi-fidelity computer experiments such as the heat exchanger problem described in (Qian et al., 2006).

Table 6: Nested Latin hypercube designs in two-dimensional space

Level 3	(0.166670,0.863640), (0.712120,0.318180),
Level 2	(0.166670,0.863640), (0.712120,0.318180), (0.590910,0.712120), (0.984850,0.590910), (0.863640,0.984850), (0.045455,0.166670), (0.439390,0.045455), (0.287880,0.469700),
Level 3	(0.166670,0.863640), (0.712120,0.318180), (0.590910,0.712120), (0.984850,0.590910), (0.863640,0.984850), (0.045455,0.166670), (0.439390,0.045455), (0.287880,0.469700), (0.954550,0.409090), (0.833330,0.681820), (0.196970,0.136360), (0.348480,0.924240), (0.681820,0.954550), (0.651520,0.530300), (0.136360,0.378790), (0.530300,0.439390), (0.893940,0.833330), (0.621210,0.075758), (0.318180,0.772730), (0.257580,0.287880), (0.772730,0.106060), (0.075758,0.742420), (0.378790,0.196970), (0.106060,0.560610), (0.560610,0.227270), (0.803030,0.500000), (0.469700,0.621210), (0.227270,0.651520), (0.924240,0.257580), (0.409090,0.348480), (0.500000,0.893940), (0.742420,0.803030),

Acknowledgement

The authors are grateful for the AE and reviewers for very helpful comments. This research is supported by NSF DMS-1914636, DMS-2312173, and CNS-2328395.

References

T. Santner, B. Williams, W. Notz, The Design and Analysis of Computer Experiments, Springer Verlag, 2003.

Table 7: Results for the proposed MLGP method and the single-level design method in higher dimensional cases

	$d = 4$		$d = 8$	
	Avg. RMSE	Structure	Avg. RMSE	Structure
MLGP	0.3702	24, 10, 5	1.074	12, 9, 6
Single-level	0.4621	0, 0, 9	1.181	0, 0, 9

- R. B. Gramacy, *Surrogates: Gaussian process modeling, design, and optimization for the applied sciences*, Chapman and Hall/CRC, 2020.
- P. Z. Qian, C. J. Wu, Bayesian hierarchical modeling for integrating low-accuracy and high-accuracy experiments, *Technometrics* 50 (2008) 192–204.
- S. Xiong, P. Z. Qian, C. J. Wu, Sequential design and analysis of high-accuracy and low-accuracy computer codes, *Technometrics* 55 (2013) 37–46.
- M. C. Kennedy, A. O’Hagan, Predicting the output from a complex computer code when fast approximations are available, *Biometrika* 87 (2000) 1–13.
- G. Pilania, J. E. Gubernatis, T. Lookman, Multi-fidelity machine learning models for accurate bandgap predictions of solids, *Computational Materials Science* 129 (2017) 156–163.
- K. Cutajar, M. Pullin, A. Damianou, N. Lawrence, J. González, Deep gaussian processes for multi-fidelity modeling, *arXiv preprint arXiv:1903.07320* (2019).
- R. Tuo, C. J. Wu, D. Yu, Surrogate modeling of computer experiments with different mesh densities, *Technometrics* 56 (2014) 372–380.
- K. Fang, R. Li, A. Sudjianto, *Design and Modeling for Computer Experiments*, volume 6, Chapman & Hall/CRC, 2005.
- P. Z. Qian, Nested latin hypercube designs, *Biometrika* 96 (2009) 957–970.
- X. He, P. Z. Qian, Nested orthogonal array-based latin hypercube designs, *Biometrika* 98 (2011) 721–731.

- G. Rennen, B. Husslage, E. R. Van Dam, D. Den Hertog, Nested maximin latin hypercube designs, *Structural and Multidisciplinary Optimization* 41 (2010) 371–395.
- P. Z. Qian, Sliced latin hypercube designs, *Journal of the American Statistical Association* 107 (2012) 393–399.
- Y. Hwang, X. He, P. Z. Qian, Sliced orthogonal array-based latin hypercube designs, *Technometrics* 58 (2016) 50–61.
- Z. Qian, C. C. Seepersad, V. R. Joseph, J. K. Allen, C. Jeff Wu, Building surrogate models based on detailed and approximate simulations (2006).
- A. Ehara, S. Guillas, An adaptive strategy for sequential designs of multilevel computer experiments, *arXiv preprint arXiv:2104.02037* (2021).
- C.-L. Sung, Y. Ji, T. Tang, S. Mak, Stacking designs: designing multi-fidelity computer experiments with confidence, *arXiv preprint arXiv:2211.00268* (2022).
- X. He, P. Z. Qian, A central limit theorem for nested or sliced latin hypercube designs, *Statistica Sinica* (2016) 1117–1128.
- M. B. Giles, Multilevel monte carlo path simulation, *Operations research* 56 (2008) 607–617.
- M. B. Giles, Multilevel monte carlo methods, *Acta numerica* 24 (2015) 259–328.
- S. Heinrich, Multilevel monte carlo methods, in: *International Conference on Large-Scale Scientific Computing*, Springer, 2001, pp. 58–67.
- L. W. Ng, K. E. Willcox, Multifidelity approaches for optimization under uncertainty, *International Journal for numerical methods in Engineering* 100 (2014) 746–772.
- A.-L. Haji-Ali, F. Nobile, R. Tempone, Multi-index monte carlo: when sparsity meets sampling, *Numerische Mathematik* 132 (2016) 767–806.
- B. Peherstorfer, T. Cui, Y. Marzouk, K. Willcox, Multifidelity importance sampling, *Computer Methods in Applied Mechanics and Engineering* 300 (2016a) 490–509.

- B. Peherstorfer, K. Willcox, M. Gunzburger, Optimal model management for multifidelity monte carlo estimation, *SIAM Journal on Scientific Computing* 38 (2016b) A3163–A3194.
- G. Geraci, M. S. Eldred, G. Iaccarino, A multifidelity multilevel monte carlo method for uncertainty propagation in aerospace applications, in: 19th AIAA non-deterministic approaches conference, 2017, p. 1951.
- A. L. Teckentrup, P. Jantsch, C. G. Webster, M. Gunzburger, A multilevel stochastic collocation method for partial differential equations with random input data, *SIAM/ASA Journal on Uncertainty Quantification* 3 (2015) 1046–1074.
- R. Tuo, W. Wang, Kriging prediction with isotropic Matérn correlations: Robustness and experimental designs., *J. Mach. Learn. Res.* 21 (2020) 187–1.
- A. I. Forrester, A. Sóbester, A. J. Keane, Multi-fidelity optimization via surrogate modelling, *Proceedings of the royal society a: mathematical, physical and engineering sciences* 463 (2007) 3251–3269.
- M. Kennedy, A. O’Hagan, Bayesian calibration of computer models, *Journal of the Royal Statistical Society: Series B* 63 (2001) 425–464.
- A. Wilson, R. Adams, Gaussian process kernels for pattern discovery and extrapolation, in: *International conference on machine learning*, PMLR, 2013, pp. 1067–1075.
- E. Schulz, M. Speekenbrink, A. Krause, A tutorial on gaussian process regression: Modelling, exploring, and exploiting functions, *Journal of Mathematical Psychology* 85 (2018) 1–16.
- J. H. Halton, Algorithm 247: Radical-inverse quasi-random point sequence, *Communications of the ACM* 7 (1964) 701–702.
- D. Chen, S. Xiong, Flexible nested latin hypercube designs for computer experiments, *Journal of Quality Technology* 49 (2017) 337–353.

Appendix A. Proofs for Theorem 1-3

In this section, we prove Theorem 1-3.

Appendix A.1. Proof of Theorem 1

Proof. By definition,

$$\begin{aligned}\hat{y}_K(x) &= \mathbb{E} \left[\sum_{i=0}^K \delta_i(x) \middle| y_K(\mathcal{X}_K), \dots, y_0(\mathcal{X}_0) \right] \\ &= \sum_{i=0}^K \mathbb{E} \left[\delta_i(x) \middle| y_K(\mathcal{X}_K), \dots, y_0(\mathcal{X}_0) \right]\end{aligned}$$

Because δ_i 's are mutually independent, for each i we can get

$$\begin{aligned}& \mathbb{E} \left[\delta_i(x) \middle| y_K(\mathcal{X}_K), \dots, y_0(\mathcal{X}_0) \right] \\ &= \mathbb{E} \left[\delta_i(x) \middle| y_K(\mathcal{X}_K) - y_{K-1}(\mathcal{X}_k), \dots, y_1(\mathcal{X}_1) - y_0(\mathcal{X}_0), y_0(\mathcal{X}_0) \right] \\ &= \mathbb{E} \left[\delta_i(x) \middle| y_i(\mathcal{X}_i) - y_{i-1}(\mathcal{X}_i) \right].\end{aligned}$$

Then we can rewrite the $\hat{y}_K(x)$ as

$$\hat{y}_K(x) = \sum_{i=0}^K \mathbb{E} \left[\delta_i(x) \middle| y_i(\mathcal{X}_i) - y_{i-1}(\mathcal{X}_i) \right].$$

□

Appendix A.2. Proof of Theorem 2

Proof. By definition,

$$\begin{aligned}
\mathbb{E} \|y_K - y_\infty\|_{L_2}^2 &= \mathbb{E} \left\| \sum_{i=K+1}^{\infty} \delta_i \right\|_{L_2}^2 \\
&= \sum_{i=K+1}^{\infty} \mathbb{E} \|\delta_i\|_{L_2}^2 \\
&= \sum_{i=K+1}^{\infty} \mathbb{E} \left(\int_{\mathfrak{X}} \delta_i^2 dx \right) \\
&= \sum_{i=K+1}^{\infty} \int_{\mathfrak{X}} \mathbb{E}(\delta_i^2) dx \\
&= \sum_{i=K+1}^{\infty} C_s \lambda^{2i} \sigma^2 \\
&= C_l^2 \lambda^{2K} \sigma^2,
\end{aligned}$$

where \mathfrak{X} denotes the input domain of x , C_s is the area of \mathfrak{X} and constant $C_l = \sqrt{C_s}/(1 - \lambda)$. \square

Appendix A.3. Proof of Theorem 4

Proof. Based on the Theorem 1, we have

$$\begin{aligned}
\mathbb{E} \|y_K - \hat{y}_K\|_{L_2}^2 &= \mathbb{E} \left\| \sum_{i=0}^k (I_i(\delta_i) - \delta_i) \right\|_{L_2}^2 \\
&= \int_{\mathfrak{X}} \sum_{i=0}^k (I_i(\delta_i) - \delta_i)^2 dx \\
&= \int_{\mathfrak{X}} \sum_{i=0}^k \mathbb{E}((I_i(\delta_i) - \delta_i)^2) dx \\
&\leq \sum_{i=0}^k p \sigma^2 \lambda^{2i} n_i^{-\nu/d},
\end{aligned}$$

where n_i is the number of samples in the i -th step, p is a constant only based on the correlation function, d is the dimension of the input space and ν is a constant. \square

Appendix B. Solve the optimization problem

Consider the optimization problem

$$\min_{n_i} \sum_{i=0}^K n_i C_i \quad (\text{B.1})$$

$$\text{s.t.} \quad \sum_{i=0}^K \lambda^{2i} \sigma^2 n_i^{-\nu/d} \leq \epsilon^2/2 \quad (\text{B.2})$$

We form the Lagrange function of (B.1) as

$$L(n_0, n_1, \dots, n_K, \eta) = \sum_{i=0}^K n_i C_a a^i + \eta \left(\sum_{i=0}^K p \lambda^{2i} \sigma^2 n_i^{-\nu/d} - \epsilon^2/2 \right).$$

To find a local optimum, we need to have $\nabla L = 0$, leading to $K + 2$ conditions

$$\frac{\partial L}{\partial n_i} = C_a a^i - \frac{p\eta\nu}{d} \lambda^{2i} \sigma^2 n_i^{-(\nu/d+1)} = 0, \quad i = 0, 1, \dots, K \quad (\text{B.3})$$

$$\frac{\partial L}{\partial \eta} = \sum_{i=0}^K p \lambda^{2i} \sigma^2 n_i^{-\nu/d} - \epsilon^2/2 = 0. \quad (\text{B.4})$$

Solving the $(K + 1)$ equations in (B.3) leads to

$$n_i = \left(\frac{p C_a d}{\nu \sigma^2} \frac{a^i}{\lambda^{2i}} \eta^{-1} \right)^{-\frac{d}{d+\nu}}, \quad i = 0, 1, \dots, K. \quad (\text{B.5})$$

Substitute (B.5) into (B.4). Then we have

$$\eta = \frac{C_a d}{\nu} (\sigma^2)^{\frac{d}{\nu}} \left(\frac{p \epsilon^2}{2S} \right)^{-\frac{d+\nu}{\nu}}, \quad (\text{B.6})$$

where

$$S = \sum_{i=0}^K (a^i)^{\frac{\nu}{d+\nu}} (\lambda^{2i})^{\frac{d}{d+\nu}}.$$

Substitute (B.6) into (B.5). We get

$$n_i = \left(\frac{\epsilon^2}{2p\sigma^2 S}\right)^{-\frac{d}{\nu}} \left(\frac{a^i}{\lambda^{2i}}\right)^{-\frac{d}{d+\nu}}, \quad i = 0, 1, \dots, K.$$

Since n_i is an integer, we choose

$$n_i^* = \lceil n_i \rceil$$

to get an approximate solution to the original problem.

Appendix C. Analysis of cost for the MLGP

In this section, we make the analysis of the cost based on the K and n_i^* given in the above section. The total cost is given by

$$C_\epsilon = \sum_{i=0}^K n_i^* C_i \leq \sum_{i=0}^K n_i^* C_a a^i.$$

Since $\lceil n_i \rceil \leq n_i + 1$, we have

$$\begin{aligned} C_\epsilon &\leq \sum_{i=0}^K C a (n_i + 1) a^i \\ &\approx \sum_{i=0}^K (S\sigma^2(\epsilon^2/2)^{-1})^{\frac{d}{\nu}} \sum_{i=0}^K (a^{\frac{\nu}{d+\nu}} \lambda^{\frac{2d}{d+\nu}})^i + \sum_{i=0}^K a^i \\ &= (2\sigma^2\epsilon^{-2})^{\frac{d}{\nu}} S^{\frac{d+\nu}{\nu}} + \sum_{i=0}^K a^i. \end{aligned} \tag{C.1}$$

We denote the first part on the right-hand side of (C.1) as part (I) and the second part as (II), and consider them separately.

If $(a^i)^{\frac{\nu}{d+\nu}} (\lambda^{2i})^{\frac{d}{d+\nu}} = 1$ (i.e., $\alpha\nu = d\beta$), then

$$\begin{aligned} (I) &= (2\sigma^2\epsilon^{-2})^{\frac{d}{\nu}} (K+1)^{\frac{d+\nu}{\nu}} \\ &\simeq \epsilon^{-2d/\nu} (2 \log_{\lambda^2} \frac{\epsilon}{2C_l\sigma})^{\frac{d+\nu}{\nu}} \\ &\simeq \epsilon^{-2d/\nu} |\ln \epsilon^2|^{\frac{d+\nu}{\nu}}; \end{aligned}$$

$$\begin{aligned} (II) &= \frac{a^K(1-a^{-(K+1)})}{1-a^{-1}} \\ &\simeq a^K \simeq (\epsilon^2)(\ln a / \ln \lambda^2) \\ &= \epsilon^{-2d/\nu}. \end{aligned}$$

Since $\epsilon^{-2d/\nu} |\ln \epsilon^2|^{\frac{d+\nu}{\nu}} > \epsilon^{-2d/\nu}$, $C_\epsilon \lesssim \epsilon^{-2d/\nu} |\ln \epsilon^2|^{\frac{d+\nu}{\nu}}$.

If $(a^i)^{\frac{\nu}{d+\nu}} (\lambda^{2i})^{\frac{d}{d+\nu}} < 1$ (i.e., $\alpha\nu < d\beta$), S will converge to a limitation which is independent of K . As a result, we have

$$(I) \lesssim \epsilon^{-2d/\nu};$$

$$(II) \lesssim \epsilon^{-2\alpha/\beta}.$$

Since $d/\nu > \alpha/\beta$, $C_\epsilon \lesssim \epsilon^{-2d/\nu}$.

If $(a^i)^{\frac{\nu}{d+\nu}} (\lambda^{2i})^{\frac{d}{d+\nu}} > 1$ (i.e., $\alpha\nu > d\beta$), we have

$$\begin{aligned} (I) &\lesssim \epsilon^{-2d/\nu} \left(\exp \frac{\alpha\nu - d\beta}{d+\nu} \right)^{\frac{K(d+\nu)}{\nu}} \\ &\lesssim \epsilon^{-2d/\nu} \exp \left(-\frac{(\ln \epsilon^2)(\alpha\nu - d\beta)}{\nu\beta} \right) \\ &= \epsilon^{-2\alpha/\beta}; \end{aligned}$$

$$(II) \simeq \epsilon^{-2\alpha/\beta}.$$

As a result, $C_\epsilon \lesssim \epsilon^{-2\alpha/\beta}$.

In summary,

$$C_\epsilon \lesssim \begin{cases} \epsilon^{-2d/\nu}, & \alpha\nu < d\beta \\ \epsilon^{-2d/\nu} |\ln \epsilon^2|^{\frac{d+\nu}{\nu}}, & \alpha\nu = d\beta \\ \epsilon^{-2\alpha/\beta}, & \alpha\nu > d\beta \end{cases}$$

Appendix D. Analysis of cost for single-level

The error caused by single-level approximation can be bounded as

$$\mathbb{E}(\|y_\infty - \hat{y}_K^{SL}\|^2) = \mathbb{E}(\|y_\infty - y_K^{SL}\|^2 + \|y_K^{SL} - \hat{y}_K^{SL}\|^2),$$

where $\hat{y}_K^{SL} = I(\delta_K)$. Then the objective function for this single-level approximation can be summarized as

$$2 \min_{K, n_K} n_K C_K \tag{D.1}$$

$$\text{s.t. } \mathbb{E} \|y_\infty - \hat{y}_K^{SL}\|_{L^2}^2 \leq \epsilon \tag{D.2}$$

Based on Theorems 1 and 2, we have

$$\mathbb{E} \|y_\infty - \hat{y}_K^{SL}\|^2 \gtrsim \lambda^{2K} \sigma^2 + \sigma^2 n_K^{-\nu/d},$$

where n_K is the number of samples. It should be sufficient to bound the upper bound of the error by ϵ , that is,

$$\lambda^{2K} + n_K^{-\nu/d} \lesssim \epsilon^2. \tag{D.3}$$

From the (D.3), we can get the lower bound for n_K , that is,

$$n_K \gtrsim (\epsilon^2 - \lambda^{2K})^{-d/\nu}.$$

Then we have the lower bound for the cost of single-level approximation:

$$C_\epsilon^{SL} = n_K C_k \gtrsim a^K (\epsilon^2 - \lambda^{2K})^{-d/\nu}. \tag{D.4}$$

We denote $a = \exp(\alpha)$ and $\lambda^2 = \exp(-\beta)$ for convenience, $\alpha, \beta > 0$. Then we can rewrite (D.4) as

$$\ln C_\epsilon^{SL} \gtrsim \alpha K - \frac{d}{\nu} \ln(\epsilon^2 - e^{-\beta K}). \tag{D.5}$$

Now we want to find the lower bound of C_ϵ^{SK} , that is, we need to find the lower bound for the right-hand side of (D.5). Consider the following function with respect to K :

$$T(K) = \alpha K - \frac{d}{\nu} \ln(\epsilon^2 - e^{-\beta K}).$$

Set the derivative of T with respect to K equal to 0:

$$\frac{dT}{dK} = \alpha + \frac{d\beta}{\nu} \left(1 - \frac{\epsilon^2}{\epsilon^2 - e^{-\beta K}}\right) = 0.$$

We can get the solution $K_0 = -\frac{1}{\beta} \ln \frac{\epsilon^2 \alpha \nu}{\alpha \nu + \beta d}$. When $K < K_0$, $T(K)$ is decreasing and when $K > K_0$, $T(K)$ is increasing. Substitute $K = 0$ into $T(K)$, we can get the lower bound of the cost for the single-level:

$$C_\epsilon^{SL} \gtrsim \epsilon^{-2(\frac{d}{\nu} + \frac{\alpha}{\beta})}.$$